SACLANTCEN REPORT
serial no: SR-246

SACLANT UNDERSEA
RESEARCH CENTRE
REPORT

DEDUCTION OF SYNTHETIC TEMPERATURE PROFILES FROM SST OBSERVATIONS IN THE ICELAND-FAEROE FRONTAL REGION

A. Warn-Varnas, H.H. Essen,
E. Gezgin

January 1996

The SACLANT Undersea Research Centre provides the Supreme Allied Commander Atlantic (SACLANT) with scientific and technical assistance under the terms of its NATO charter, which entered into force on 1 February 1963. Without prejudice to this main task – and under the policy direction of SACLANT – the Centre also renders scientific and technical assistance to the individual NATO nations.

SACLANT Undersea Research Centre
Viale San Bartolomeo 400
19138 San Bartolomeo (SP), Italy

tel: +39-187-540.111
fax: +39-187-524.600

e-mail: library@saclantc.nato.int

NORTH ATLANTIC TREATY ORGANIZATION

Report no.changed (Mar 2006): SR-246-UU

Deduction of synthetic temperature profiles from SST observations in the Iceland-Faeroe frontal region

A. Warn-Varnas, H.-H. Essen, E. Gezgin

The content of this document pertains to work performed under Project 04 of the SACLANTCEN Programme of Work. The document has been approved for release by The Director, SACLANTCEN.

David L. Bradley
Director

intentionally blank page

Deduction of synthetic temperature profiles from SST observations in the Iceland-Faeroe frontal region

A. Warn-Varnas, H.-H. Essen, E. Gezgin[1]

Executive Summary: Satellite data form an important extension to conventional oceanographic data by providing large area coverage with, in some cases, high resolution. Satellite remote sensing is a highly appropriate technique for the rapid assessment of unknown areas which has become one of the main research tasks at SACLANTCEN in recent years. For rapid environmental assessment, increasing attention has been paid to correlating satellite surface measurements with the subsurface structure of the oceans.

Most of the satellite data used at SACLANTCEN originate from the Advanced Very High Resolution Radiometer (AVHRR) on US weather satellites. These satellites take measurements in the visible and infrared parts of the spectrum, which can be used to generate sea-surface temperature (SST) maps with an optimum resolution of 1 km^2. A method has been developed to extract information on subsurface sound-speed from satellite-measured SST. The method is based on the decomposition of vertical sound-speed profiles into a few characteristic functions. It has been demonstrated that for the Iceland-Faeroe Frontal (IFF) area, the amplitude of the dominant function can be derived from SST, and that this function represents important features of subsurface sound speed. However, data from Mediterranean coastal areas were analysed using the same method with successful results for only one of four data sets.

This report continues the work with a data set extending to greater depths than those used before. Hydrographic data from the October 1992 IFF survey is used to determine the characteristic functions and satellite-measured SST for the construction of synthetic temperature profiles. Average errors were computed for synthetic temperature profiles in typical water categories. Corrections to the processed satellite SST data had to be applied using surface drifter data and sensitivity tests.

The work demonstrates that it is feasible to derive synthetic temperature profiles and sound speed distributions below the surface from SST observations in some sections of a dynamic frontal region. The approach can be extended to other times of the year and seasons for which regional *in situ* data is available.

[1] Department of Navigation, Hydrography and Oceanography, 81647 Çubuklu, Istanbul, Turkey

intentionally blank page

Deduction of synthetic temperature profiles from SST observations in the Iceland-Faeroe frontal region

A. Warn-Varnas, H.-H. Essen, E. Gezgin[1]

Abstract: Subsurface temperature and sound speed profiles are generated from satellite SST observations and validated by hydrocast observations. Hydrographic data from the October 1992 Iceland Faeroe frontal survey is used for the calculation of Empirical Orthogonal Functions (EOFs). Statistical relationships between the EOF amplitudes and SSTs are derived and used for the construction of synthetic temperature profiles and sound speed distributions in the ocean. Average Root-Mean Square (RMS) errors were computed for synthetic temperature profiles in typical water categories. Corrections to the processed satellite SST data were applied using surface drifter data and sensitivity tests.

The survey data reflects the water mass structure in three distinct regions; Atlantic, Frontal and Arctic, for which characteristic TS curves are derived. The best agreement between the synthetically generated temperature profiles, from SST data, with CTD measurements occurs in the Arctic region where a tendency to follow the slope and magnitude *versus* depth exists. The Frontal region shows disagreements in the upper thermocline with agreement elsewhere. In the Atlantic region there is agreement only in the upper mixed layer. In the thermocline regime the slope exhibits a parallel offset relative to the data. The differences are attributed to the inherent errors of EOF reconstruction which peak in the thermocline and the scatter of EOF amplitudes *versus* SST measurements.

The work demonstrates that it is possible to derive synthetic temperature and sound speed profiles in the ocean from SST observations of particular water mass configurations at certain times of the season.

Keywords: Iceland-Faeroe frontal region – sea-surface temperature – temperature profiles

[1] Department of Navigation, Hydrography and Oceanography, 81647 Çubuklu, Istanbul, Turkey

Contents

Acknowledgements: Thanks go to the Captain and crew of NATO Research Vessel *Alliance*. The CTD data were collected and processed by the Ocean Engineering Department (OED) and Applied Oceanography Group (AOG) at SACLANTCEN. Dr. A. Miller provided the interpolated data set and E. Nacini processed the AVHRR image.

1
Introduction

This study examines the derivation of synthetic temperature profiles in the Iceland-Faeroe Frontal (IFF) region from satellite remotely sensed sea surface temperature (SST) data, in characteristically distinct regional water masses. The temperature structures deduced allow the calculation, for acoustic purposes, of spatial and temporal sound speed variability.

The most successful approach for constructing synthetic temperature profiles *versus* depth uses correlation between subsurface temperatures and dynamic height. Cheney [1] and Khedouri *et al.* [2] observed a high degree of correlation between the dynamic height and subsurface temperature profiles in the Gulf Stream. This was pursued by deWitt [3] in the Gulf Stream and Kuroshio regions. He compiled a monthly database of temperature and salinity hydrocasts, calculated the Empirical Orthogonal Functions (EOFs), and derived (for the first time) the statistical relationships between EOF amplitudes and dynamic height. This method allowed the calculations of synthetic temperature profiles from dynamic heights or sea surface elevations measured by altimeter. Carnes *et al.* [4] used this methodology for the calculation of synthetic temperature profiles from Geosat altimetry in the Gulf Stream, where a strong sea surface elevation signal exists. Results showed agreement with temperature cross sections measured by AXBTs.

Pistek *et al.* [5] generated weekly three-dimensional temperature and salinity distributions from sea surface topography and a Gulf Sream feature model in the Northwest Atlantic using the same approach. Boissier and Bouxin [6] performed a similar analysis in the Northeast Atlantic and obtained vertical sound speed distributions from calculated dynamic heights during the 1988 Athena experiment.

Cummings [7] generated EOFs for a seasonal global water mass model and performed regression analysis of EOF amplitudes *versus* longitude, latitude, day of the year, SST, and selected interaction terms. He found that the EOF water mass model was a better predictor of the MOODS (a data base of temperature and salinity) profiles than climatology. The accuracy of prediction was attributed to the inclusion of SST information in the regression scatter analysis of EOF amplitudes. In another context, Fiedler [8] pointed out that the correlation of sea surface temperature with subsurface structures was only partially successful. It has been suggested by Carnes *et al.* [4] that a unique dependence of subsurface structures on dynamic height is not to be expected in every region of the ocean.

In the IFF region, dynamic height is of the order of ±10 cm, the accuracy limit of presently operating space-borne altimeters, which means that these satellite data are not appropriate for the determination of subsurface structures. For this reason, Essen and Sellschopp [9] investigated the dependence of sound-speed EOFs on SST, which may also be measured from space. Using data from a CTD survey and thermistor-chain measurements they concentrated on the sound-speed distribution of the upper 150 m of the ocean and were able to reconstruct important features of subsurface sound speeds. Essen [10] applied the same method to data from coastal regions of the Mediterranean, the areas south of Elba and Sicily, and the Strait of Otranto. Satisfactory results were obtained only for the area south of Sicily.

In this report, the generation of synthetic temperature profiles, to a depth of 600 m, from sea surface signatures is studied in the context of the complex oceanography of the IFF region. The warm highly saline Atlantic water meets the cold low salinity Arctic type water in the presence of variable topography which rises to about 400 m of the surface in the form of a ridge which anchors the front. The Atlantic water overflows the Arctic type water, resulting in a mixed water mass structure at some latitude and longitude locations. A high degree of mesoscale dynamical activity exists, and as the front meanders, cold and warm eddies are formed, Niiler *et al.* [11].

The water masses in the IFF region are formed from a mixture of Atlantic and Polar water. The Arctic type water is an admixture of the two. Water mass circulation time influences their TS structure. On the surface further modifications are induced by atmospheric cooling and coastal runoff. In a recent SeaSoar study of the IFF region, seven water masses have been indentifed , Read and Pollard [12].

The present study will use hydrographic data from an experiment in the IFF region conducted by the SACLANT Undersea Research Centre with NRV *Alliance*. The cruise, which took place in October of 1992, was part of the mesoscale surveys of the IFF region oriented towards description and prediction of local dynamics.

2
Data

A series of Iceland-Faeroe Frontal (IFF) surveys was performed by SACLANT Centre in collaboration with Harvard University (USA), NRL (USA), and FWG (Germany). The surveys addressed the mesoscale structures and evolution. Shipboard descriptions and predictions of the IFF were performed, on the NRV *Alliance*, using the Harvard University data assimilation methods, objective analysis schemes, and dynamical models.

In October of 1992 a survey of the IFF was conducted for the purpose of dynamical model initialization and validation. These models evolved the mesososcale dynamics and predicted the subsequent ocean structure. The surveys consisted of CTDs, XCTDs, and XBTs. The positions of the CTD casts from the initialization array are shown in Fig. 1.

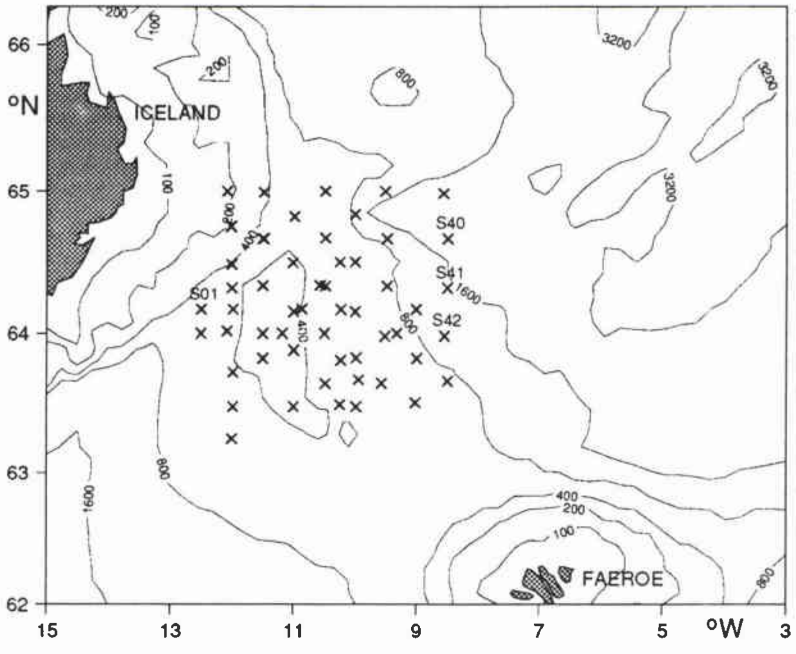

Figure 1 *Bathymetry (m) and locations of CTDs during the initialization survey. The survey was conducted from west to east during the period from 19 to 25 October 1992. Stations indicated by numbers are referred to in the subsequent analysis.*

The data from the intialization array was projected onto a three-dimensional grid with the Harvard University objective analysis scheme. This interpolation scheme is based on the Gandin [13] approach. An isotropic correlation function was used,

$$\rho(r) = (1 - \frac{r}{A})exp(-\frac{r^2}{2B^2}), \tag{1}$$

where r is the separation in km, $A = 60km$ is the zero crossing, and $B = 10km$ is the decay. Other input parameters involve an objective analysis error level and a radius of influence that controls the number of observations in the analysis, Carter and Robinson [14] and Miller *et al.* [15]. The horizontal grid spacing was 5 km. The vertical spacing was 5 m in the top 30 m, 10 m between 30 m and 50 m, 25 m between 50 m and 400 m, and 50 m between 400 m and 600 m. Objective analysis was performed independently at each vertical level.

In some instances the vertical depth of interest will terminate at 400 m below the surface, the ridge location. In others, the depth of interest will extend to 600 m with some of the casts subjected to exponential extrapolation, Miller *et al.* [15].

3 Analytical Methodology

The measured vertical temperature profiles are expanded using EOF basis functions,

$$T_{ln} = T_{l0} + \sum_{m=1}^{M} a_n^{(m)} e_l^{(m)}. \tag{2}$$

Here $l = 1, ..., L$ counts the depth horizons at which temperature measurements have been taken, and $n = 1, ..., N$ the locations of the CTD casts. T_{l0} is the mean temperature at depth level l, averaged over all casts. The order of the EOF is given by $m = 1, ..., M \leq L$. Normally, a small number of modes contains most of the variance and summation over m may be restricted to values considerably smaller than L. The $e_l^{(m)}$ are eigenfunctions of the covariance matrix of the deviation temperatures, and the amplitudes $a_n^{(m)}$ in Eq. (2) are determined by,

$$a_n^{(m)} = \sum_{l=1}^{L} (T_{ln} - T_{l0}) e_l^{(m)}. \tag{3}$$

The EOF eigenvalues account for the amount of variance as explained by the modes.

DeWitt [3] first detected a strong dependence of EOF amplitudes on dynamic height for the Gulf Stream area. Although the sea surface topography shows much smaller excursions from the mean in the Iceland-Faeroe area, these relations are also found in the data under investigation. In order to quantify this dependence, a regression analysis is performed by approximating the EOF amplitudes through a polynomial of order K,

$$a_n \approx A_o + \sum_{k=1}^{K} A_k x_n^k, \tag{4}$$

where x_n is the dynamic height or sea-surface temperature at position n. The coefficients A_k are determined by a least-squares fit, which is performed for each significant EOF mode separately. The quality of the approximation may be described by the coefficient of determination,

$$r^2 = \frac{s^2 - \epsilon^2}{s^2} \quad with, \; \epsilon^2 = \sum_{n=1}^{N} [a_n - (A_o + \sum_{k=1}^{K} A_k x_n^k)]^2, \tag{5}$$

where s^2 is the variance of the amplitudes a_n. In the case of linear regression $(K = 1)$, r is the correlation coefficient.

4

Synthetic Temperature Profiles and Interpretations

The Iceland-Faeroe Front separates the warm saline Atlantic water from the cold low salinity Arctic type water. The front has a pronounced SST signature, as sensed by the NOAA-11 satellite on 24 October 1992 (Fig. 2). A high degree of mesoscale dynamical activity is indicated by frontal meanders and the formation of cold and warm eddies. The warm highly saline Atlantic water overflows the cold low salinity Arctic water resulting in a front which tilts with depth and is anchored on the ridge, Read and Pollard [12]. Below the surface the front gradually moves south from its satellite sensed SST signature.

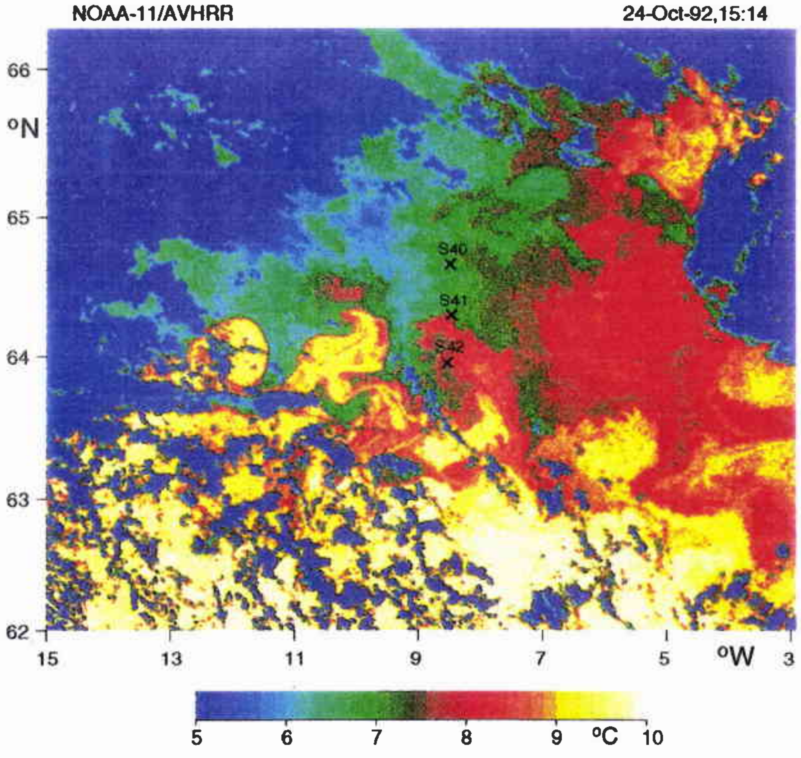

Figure 2 *Sea-surface temperature distribution sensed by NOAA-11 on 24 October 1992. The correction algorithm of Minnett [16] was applied. Dark blue, i.e. temperature below 5°C, indicates cloud coverage.*

4.1 EOFs for the data region

Empirical Orthogonal Functions (EOFs) were calculated for the set of temperature profiles generated by objective analysis of CTD data on the selected three-dimensional grid. A vertical plot of every 20th temperature profile is shown in conjunction with the 1st, 2nd and 3rd EOF in Fig. 3. The amplitude of the 1st EOF displays maximum value at a vertical distance corresponding to the largest temperature variability or variance between Atlantic and Arctic type water masses. The EOF representation reduces this variability. 2nd and 3rd EOFs produce the expected oscillations in amplitude near the zero axis displaying reduced variance. The first two EOFs account for 97% of temperature variance, a result comparable to that of Cummings [7].

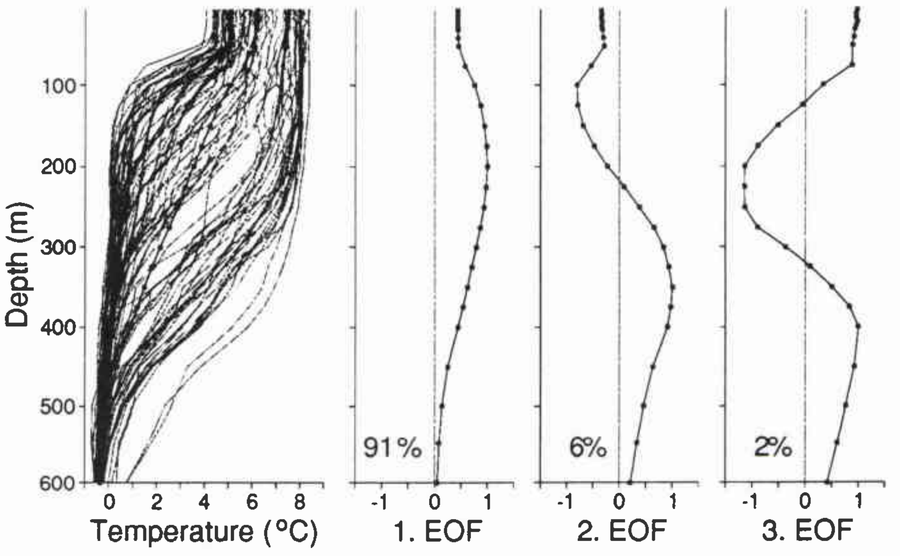

Figure 3 *From left to right: vertical plot of every 20th temperature profile, 1st, 2nd, and 3rd EOF (with indicated variance).*

4.2 Water masses and structures

Read and Pollard [12] surveyed the IFF region with a SeaSoar. Analysis of their TS diagrams indicated the presence of seven water masses. Their results on water mass categories are reproduced in Table 1. Our TS diagrams support their conclusions.

Water mass	Temperature (°C)	Salinity (ppt)
North Atlantic	> 8.0	> 35.00
Modified North Atlantic	7.5 – 8.0	35.20 – 35.25
Norwegian North Atlantic	3.0	34.98
Arctic Intermediate	0.0	34.90
Norwegian Sea Deep	−0.5	34.92
East Icelandic Current	8.0	34.30
East Icelandic	0.4	34.74

Table 1 *Water mass characteristics (from: Read and Pollard [12]).*

The region is devided into three sections, consisting of the areas south, north, and in the front. Each section will consist of various water masses or their mixtures, referred to as the Atlantic, Frontal, and Arctic regions. We have chosen the 7.4°C and 5.4°C isotherms at 5 m depth as the southern and northern boundaries of the front (Fig. 4a). This defines the frontal boundaries with respect to the surface signature of the front as would be sensed by a satellite. At depth the front moves south (Fig. 4b) as a consequence of the overflow of the Atlantic water over the Arctic. As a result a particular water column in the overflow region will contain Atlantic water on top and Arctic underneath with an intervening front. The warm and cold eddies visible in the objectively analysed temperatures are not treated separately as they are perturbations in their respective areas.

The horizontally averaged temperature and salinity distributions for the Atlantic, Frontal, and Arctic regions have been calculated. A TS water mass model was derived for each category to a depth of 600 m (Fig. 5) using extrapolated profiles in areas with depths less than 600 m. The mass structure TS curves are similar to those deduced by Read and Pollard [12] from typical CTD profiles in the seven water masses listed in Table 1. Our measurements, however, are taken at a different time of the year and reach deeper into the ocean than those of the SeaSoar.

The temperature scale starts at approximately 8°C which is the range of the North Atlantic and Modified Norwegian Atlantic Water. The bottom of the scale is just inside the minus temperature range. It contains the Arctic Intermediate water regime and reaches into the Norwegian Sea deep water. The top portions of the Atlantic and Frontal water mass structure curves fold back, in the upper 150 m, towards lower salinity values indicating the presence of warm less saline water. This feature is different to that of Read and Pollard [12] who observed a lesser slope change in the upper portion.

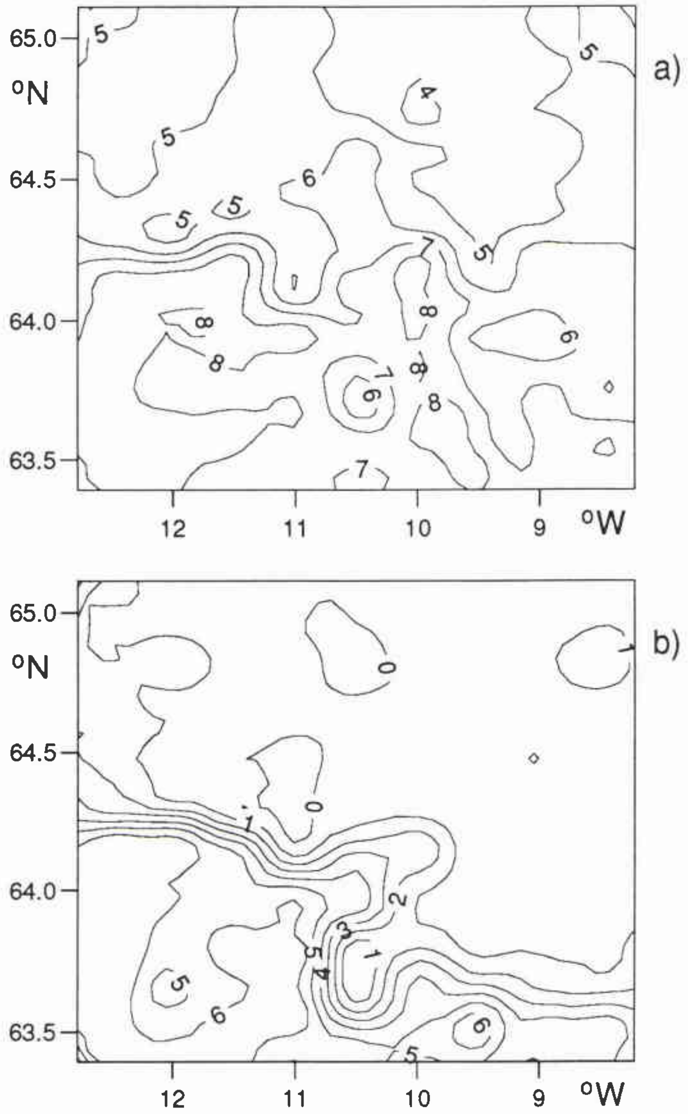

Figure 4 *Temperature distributions at: a)* 5 m, *and b)* 300 m *obtained by objective analysis of the data. The numbers refer to* °C.

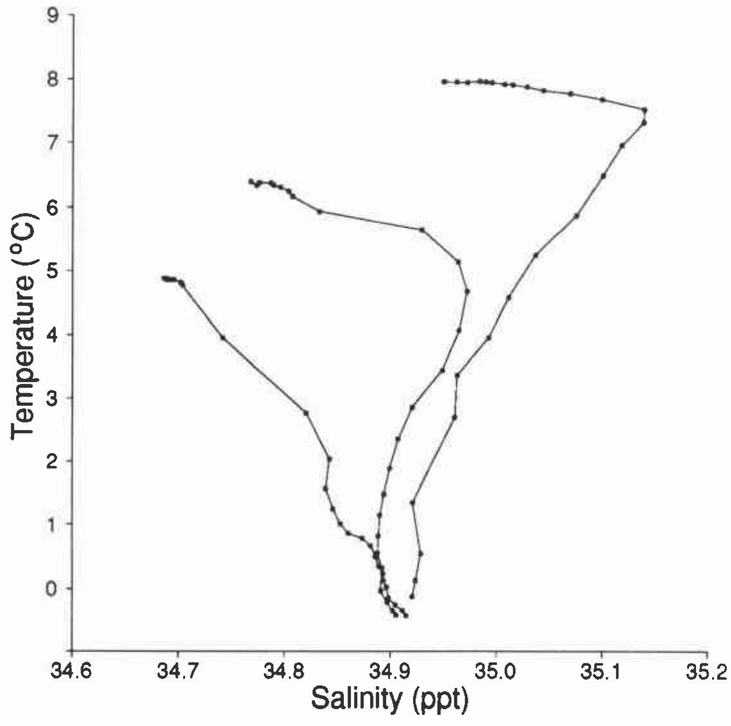

Figure 5 *From left to right: the Atlantic, Frontal, and Arctic water mass TS structures.*

4.3 Correlation of EOF amplitudes with SST

The EOF amplitudes have been correlated with the dynamic height of water columns and their sea surface temperature (SST). The calculations of dynamic height and extraction of SST were performed on every latitude and longitude grid point location used for the objective analysis. The polynomial of order K was fitted through a least squares fit as indicated in Eq. (4). Figure 6 shows the scatter diagrams of the 1st-, 2nd-, and 3rd-order EOF amplitudes *versus* dynamic height, relative to 400 m depth. Second order polynomials are used for fitting the 1st and 2nd EOF and third order for the 3rd EOF. The coefficient of determination is 0.97, 0.60, and 0.20 for the 1st, 2nd, and 3rd scatter diagrams.

Figure 7 shows the scatter diagrams for the first three EOF amplitudes *versus* SST at 5 m depth (uppermost level of the objectively analyzed CTD data). The coefficients of determination for the second order regression fits of the 1st and 2nd EOF are 0.90 and 0.35. Hence, the correlation of the EOF amplitudes is higher with dynamic height than with SST. However, the variation of dynamic height by ± 10 cm is at the limit of accuracy of space-borne altimeters. For this reason we continue our analysis with SST only.

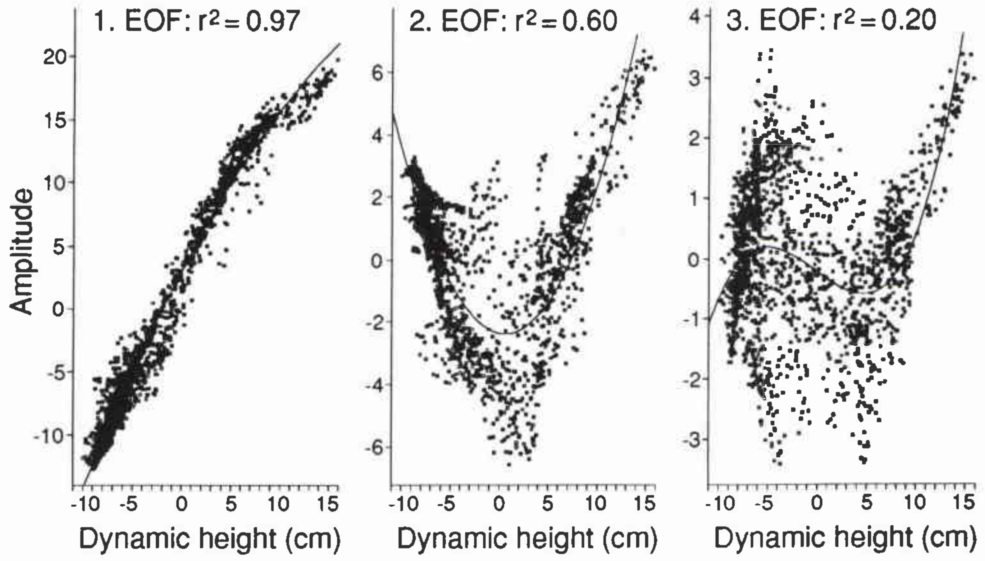

Figure 6 *Scatter diagrams of 1st, 2nd, and 3rd EOF amplitudes versus dynamic height, relative to* 400 m *depth. See Eq. (5) for definition of* r^2.

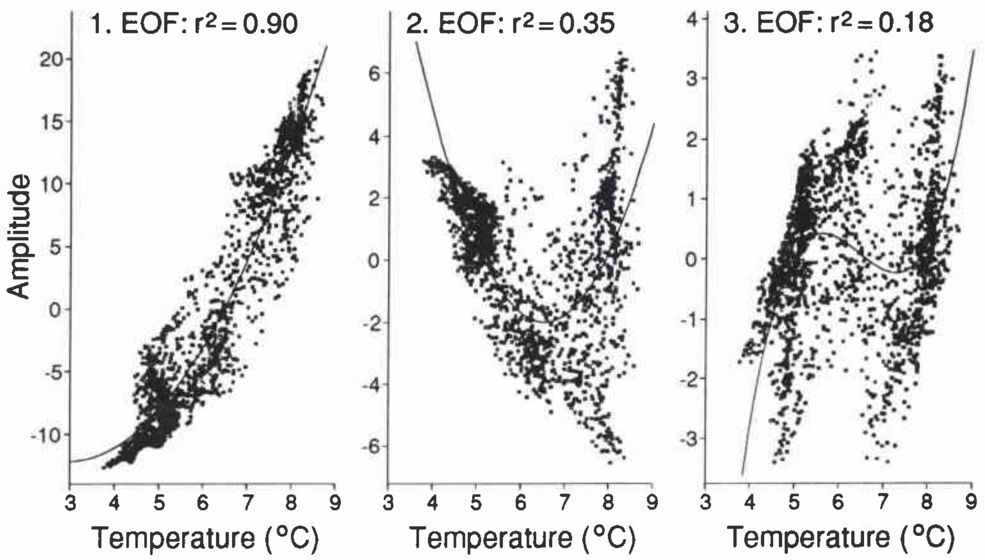

Figure 7 *Scatter diagrams of 1st, 2nd, and 3rd EOF amplitudes versus SST at* 5 m *depth. See Eq. (5) for definition of* r^2.

4.4 RMS errors for temperatures constructed from SSTs

Synthetic temperature profiles from the SST (5 m) signature (of the CTD data) have been calculated. The scatter diagram in Fig. 7 was used for relating the EOF amplitudes to SST signatures and for generating the subsurface temperature distribution by summing the first three EOFs according to Eq. (2). In order to establish the accuracy of this approach, an average RMS error distribution was derived for each of the three previously defined water mass structure regions. This was accomplished by comparing the profile constructed from SST data with the one originated from measurements. Results are shown in Fig. 8 based on SST (upper part) with RMS error for regenerating the temperature profiles from the EOF amplitudes obtained during the original EOF decomposition of the CTD profiles (lower part).

For the Arctic water mass (Fig. 8a), we note the error curves that arise when the 1st, 1st + 2nd, and 1st + 2nd + 3rd EOFs are used for reconstruction. The upper graphs refer to 5 m SST as input data. The errors for the 1st + 2nd + 3rd EOF combination show similar curves and peak in the thermocline region where temperatures exhibit greatest variability (Fig.3), around 150 m. The smallest errors are in the mixed layer region and at depth. The inherent RMS error involved in resynthesizing the profiles from the EOF basis amplitudes is shown in the lower graphs. The error decreases as more EOF functions are introduced. There is a more homogeneous distribution *versus* depth, compared to the previous case, with peaks just below the mixed layer. Inside the mixed layer the error is comparable to the SST case.

In the Frontal water mass (Fig. 8b) the RMS error for the reconstructed temperature from SST data peaks at around 250 m. This is deeper than in the Arctic water mass and spans the region of maximum temperature variability that encompasses the frontal edges (Fig. 3). Individual temperature measurements can be located at any point in the frontal envelope that contains a mixture of water masses. The inherent RMS error generated in resynthesizing the temperature profiles from EOF basis amplitudes is smaller.

For the Atlantic water mass (Fig. 8c) the RMS error for the reconstructed temperatures from SST data peaks even deeper in the ocean, at around 350 m. This is the thermocline region below mixed layer depths of around 200 m (Fig. 3). The error in all three water masses is maximum in the thermocline region. Its RMS magnitude varies from 0.5°C to almost 2.0°C. The magnitude of the RMS deviations is comparable to errors arising in the derivation of synthetic temperature profiles from dynamic heights, Carnes *et al.* [4]. There, the location of these errors is near the surface layers of the ocean, and the particular approach is used for the calculation of synthetic subsurface temperatures from satellite altimetry data.

In the Atlantic water mass, the inherent errors for calculating profiles from the EOF basis amplitudes are similar to those for other water masses.

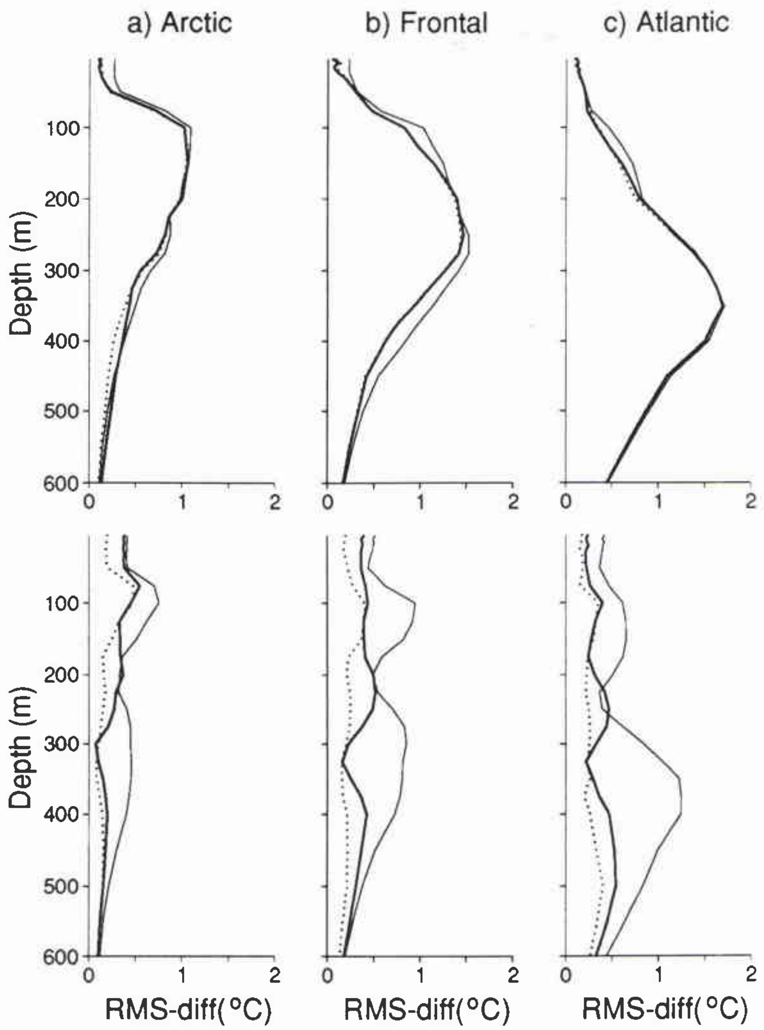

Figure 8 *Average RMS error for a) Arctic, b) Frontal , and c) Atlantic water mass structure categories in resynthesizing the temperatures from the EOF amplitudes for each water mass category. Upper graphs use SST data for reconstruction and lower graphs EOF amplitudes of the CTD data. Light solid lines indicate the use of 1st EOF only, heavy solid lines 1st plus 2nd EOF, dotted lines 1st through 3rd EOF.*

4.5 Synthetic temperature profiles in the Frontal water mass

For the calculation of synthetic temperature profiles, satellite SSTs have been chosen from the CTD locations indicated in Fig. 2. Table 2 shows the time of the CTD stations and satellite observations. Locations 41 and 42 are in the frontal water mass.

CTD station / time	satellite / time	SST	correction
40 / 24-Oct-92, 10:25	NOAA-12 / 24-Oct-92, 08:43	4.9°C	no
40 / 24-Oct-92, 10:25	NOAA-11 / 24-Oct-92, 13:33	6.9°C	-1.44°C
41 / 24-Oct-92, 13:20	NOAA-11 / 24-Oct-92, 13:33	7.5°C	-1.44°C
42 / 24-Oct-92, 16:00	NOAA-11 / 24-Oct-92, 15:14	7.8°C	-1.44°C

Table 2 *Times of CTD casts and satellite images, used for synthesizing temperature profiles.*

During the reconstructions it became evident that the satellite SSTs were not in agreement with the CTD measurements near the surface. Further research indicated that the temperatures measured by surface drifters (Poulain *et al.* [17]) were also not in agreement with SSTs derived from the NOAA-11 satellite using atmospheric correction algorithms. A scatter diagram of these results is shown in Fig. 9. The satellite observations were regressed ***versus*** surface drifter observations with a slope of one. This resulted in a bias, or difference in means, of 1.44°C with a RMS error of 0.5°C. We therefore applied a correction of -1.44°C to all NOAA-11 processed satellite SST observations (Table 2). The error is attributable to the atmospheric correction processing.

Figure 10a displays the synthetic temperature profiles calculated using the 1st, 1st + 2nd, and 1st + 2nd + 3rd EOFs at the CTD station 41. The profile derived from CTD data is indicated by circles. The most pronounced error is in the representation of the thermocline region. At depth the reconstructed profile approximates to the data. Near the surface the mixed layer structure is visible but with a temperature shift of about 0.5°C compared to the data. The sound speed profile calculated from the synthetic temperature and mean frontal salinity is shown in Fig. 10b. A surface duct exists in the mixed layer region. In the thermocline regions the sound speed decreases to a minimum around 450 m, the deep sound axis.

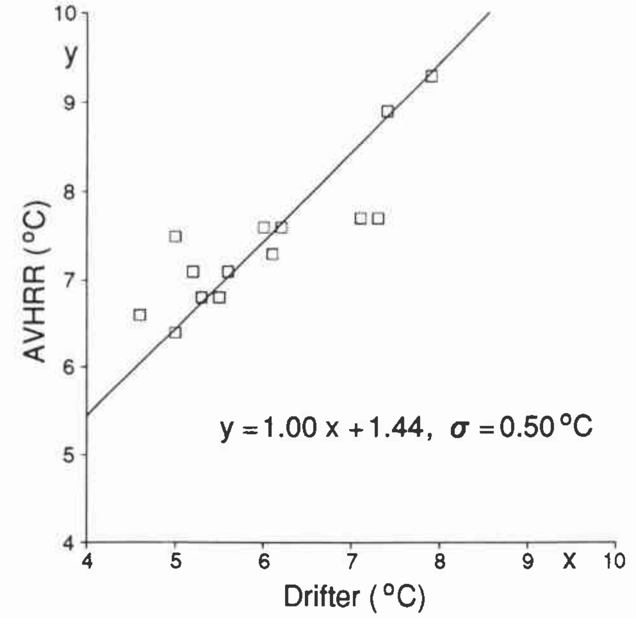

Figure 9 *Scatter diagram of satellite derived SSTs (y-axis) and SSTs measured by surface drifters on 24 October 1992 in the IFF area. The line represents linear regression with slope 1.*

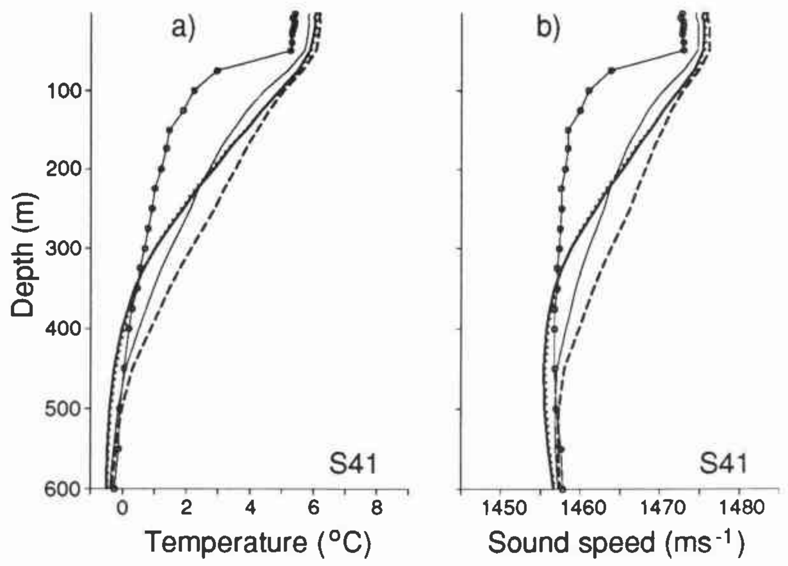

Figure 10 a) *Synthetic temperature calculated from satellite derived SSTs with 1st EOF (thin solid line), 1st plus 2nd EOF (heavy solid line), 1st through 3rd EOF (dotted line). Circles show objectively analysed data profiles, dashed lines the mean profile. b) Sound speed, calculated from temperature and a fixed salinity of* 34.85 ppt.

Experimenting with the idea of using EOF decomposition separately for each water mass category, EOFs for the Frontal water mass (defined to be between temperatures 5.4°C to 7.4°C at the surface) and the SST *versus* EOF amplitude scatter diagrams have been calculated. Then, the synthetic temperature profile was computed from the satellite SST observation at CTD station 42. Results are shown in Fig. 11b. The calculation was also performed by using the EOFs derived for the whole region as before (Fig. 11a). Some differences in results arise. In Fig. 11b, the curve indicating the use of the 1st EOF only varies only slightly in the upper ocean relative to Fig. 11a. The use of 1st + 2nd EOF has the opposite trend. This is attributable to the large scatter of the 2nd EOF amplitudes *versus* SSTs. Overall no large improvement results from the tailoring of the EOF decomposition to the frontal water mass. For the remainder of this paper, the EOF basis functions, derived for the whole region, are used.

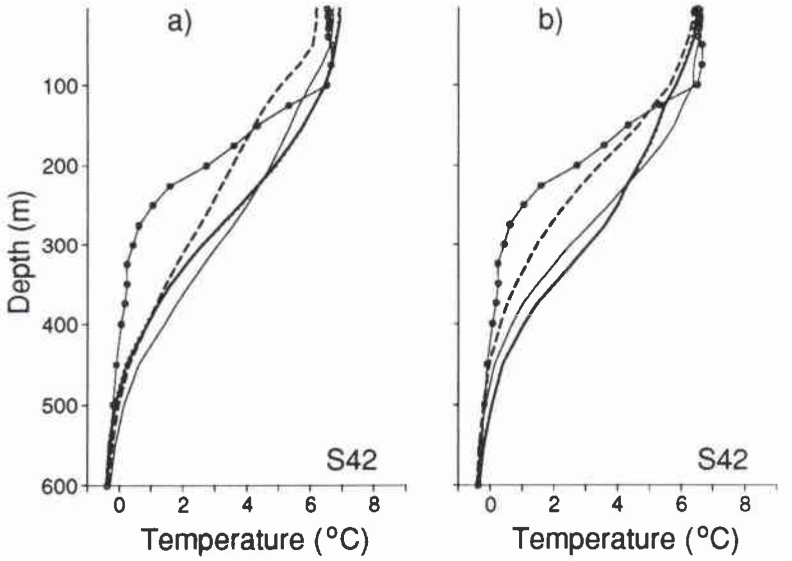

Figure 11 *Synthetic temperature calculated from satellite derived SSTs using EOFs derived from:* ***a)*** *all data,* ***b)*** *data from Frontal water mass only. Notation as in Fig. 10.*

A sensitivity study, at CTD station 41, has been performed by applying an additional correction to the SST of 0.75°C in order to move the reconstructed temperature closer to the data at the surface. The results (Fig. 12a) indicate agreement in the mixed layer and depths greater than 250 m with a slight offset in slope. In the upper thermocline, between 250 m and the bottom of the mixed layer, there is pronounced disagreement.

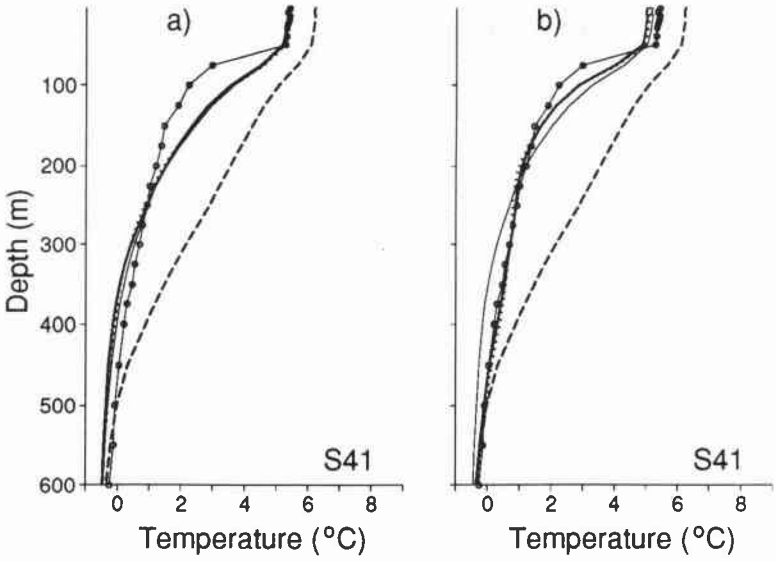

Figure 12 *Synthetic temperature calculated from: a) NOAA-11 derived SST with correction, b) EOF amplitudes derived from the data. Notation as in Fig. 10.*

The EOF amplitudes calculated from the data set were used to reconstruct the temperature profile at CTD station 41 (Fig. 12b). There is disagreement with the data in the upper thermocline and a shift of the mixed layer temperature. An inherent error in reproducing the data in the upper thermocline occurs when synthesizing Frontal region temperatures. The variability of temperature profiles is more severe than in the Atlantic or Arctic regions as pointed out in Section 4.4. In these regions the synthesized temperatures tend to diverge from the data, with the closest agreement occurring in the Arctic water.

4.6 Synthetic temperature profiles in the Arctic water mass

At CTD station 40, located in the Arctic water mass, we first constructed the synthetic temperature from the SST observations of NOAA-11 with sea surface temperature correction as indicated in Table 2. Results in Fig. 13 indicate a temperature difference relative to the data in the mixed layer and thermocline region. The difference in the mixed layer region is about 0.5°C. At depth the synthetic temperature tends to approach the data. The sound speed distribution exhibits a surface duct type structure.

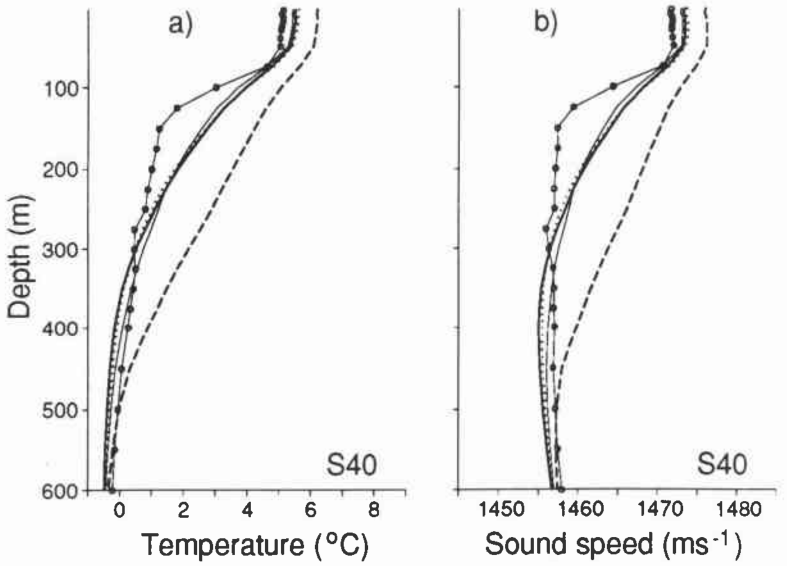

Figure 13 *a) Synthetic temperature calculated from NOAA-11 derived SST with correction, b) Sound speed, calculated from temperature and a fixed salinity of* 34.85 ppt. *Notation as in Fig. 10.*

In view of the temperature discrepancies in the mixed layer, SST data from NOAA-12 for 24 October 1992 have been considered. The observed SST value of 4.9°C was assumed to be correct and used for the temperature profile construction. Results in Fig. 14a indicated much better agreement, relative to data, in the mixed layer and thermocline regions. The synthetic sound speed profile is also close to the data (Fig. 14b). The shape of the synthetic temperature profile and its surface temperature are very sensitive to the satellite sensed SST value. This suggests a further correction of 0.5°C to the NOAA-11 measurements.

The method of constructing the synthetic temperature profiles involves the use of EOF amplitude scatter diagrams *versus* sea surface temperatures (Fig. 7). These diagrams contain an appreciable amount of scatter which translates SST errors into EOF amplitude errors. As a result the synthetic temperature profiles are sensitive to satellite SST errors.

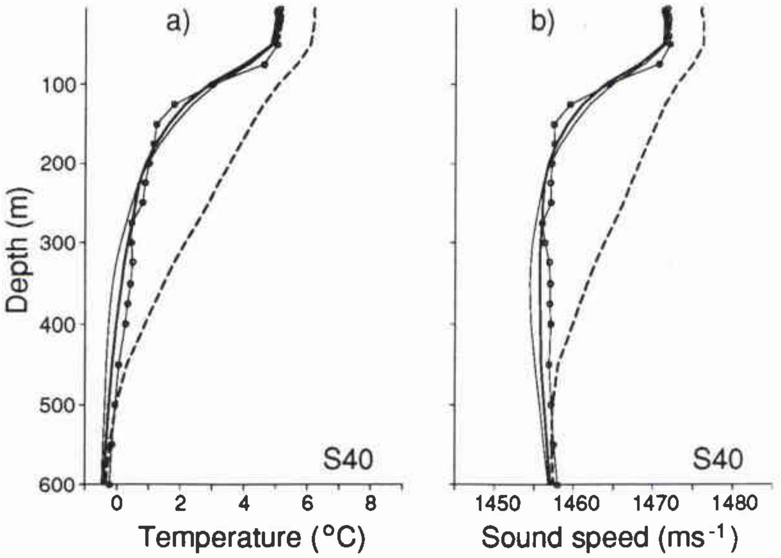

Figure 14 *Same as Fig. 13 for NOAA-12 derived SST without correction.*

4.7 Synthetic temperature profiles in the Atlantic water mass

For the Atlantic water mass calculations CTD station number 1 (Fig. 1) has been chosen. In this case the satellite derived SST was not easily accessible. Therefore, the near surface CTD temperature at 5 m was used as input. The results are shown in Fig. 15a. The reconstructed synthetic temperature profile improves with the number of EOF components included. The use of 1st + 2nd EOF yields good agreement in the upper 250 m. In the thermocline region, the synthetic slope tends to be parallel to the data but offset in magnitude towards lower temperature values. At this depth range the standard deviation of the temperatures from the mean has its largest values for data in the Atlantic water mass category. The sound speed profile (Fig. 15b) indicates a surface duct in the mixed layer region and decreasing sound speed down to 600 m.

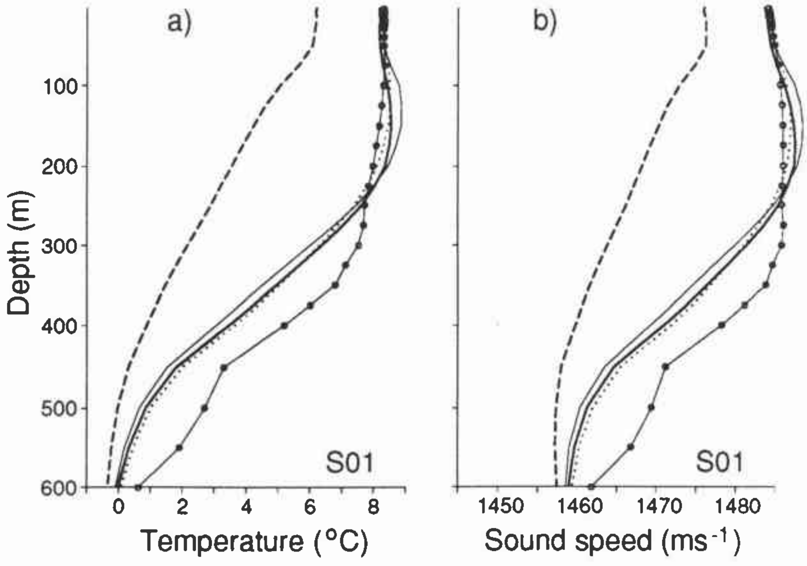

Figure 15 *a) Synthetic temperature calculated from CTD-measured SST at* 5 m *depth, b) Sound speed, calculated from temperature and a fixed salinity of* 34.85 ppt. *Notation as in Fig. 10.*

5
Conclusion

The construction of synthetic temperature profiles from sea surface observations by satellites or hydrocasts has been researched. For this purpose, the October 1992 hydrographic survey of the Iceland Faeroe Front (IFF) in conjunction with satellite observations was analysed. Empirical Orthogonal Functions (EOF) were calulated from objectively analysed subsurface temperature measurements.

Three regions of characteristic water mass mixtures were selected for the construction of synthetic temperatures from SST observations in and from the south and north of the front. For each water mass structure region, an average Root-Mean-Square (RMS) error for the synthetic temperature profiles was calculated by comparing them with the objectively analyzed data, representing ground truth. The errors ranged from 0.5°C to almost 2°C and peaked in the thermocline regions. The magnitude of the RMS deviations was comparable to the errors that arise in the derivation of synthetic temperatures from dynamic height, Carnes *et al.* [4].

During the construction of the profiles it became evident that the resultant subsurface temperature magnitude and slope is very sensitive to the correct value of SST. In most cases, the satellite derived SSTs was corrected by using surface drifter measurements as ground truth. Errors were attributed to the atmospheric correction algorithm used and perhaps some skin layer effects.

In the Frontal region, where the water masses mix together, the upper thermocline region presented the most difficulty for slope regeneration. There the synthetic profiles disagreed with data. In the mixed layer and below the upper thermocline the synthetic temperature tended to agree with data after the SST were corrected to correspond to CTD measurements of near-surface temperature. North of the front where the Arctic type of water masses occur, the synthetically constructed temperatures showed agreement, in slope and magnitude, with CTD measurements. This represented the best agreement among the three regions. In the Atlantic region south of the front, agreement existed only in the upper mixed layer. In the thermocline regime the slope exhibited a parallel offset relative to the data.

The use of EOF amplitudes, derived from CTD data, to regenerate the temperatures in the three regions was scrutinized and it was found that an inherent error occurs in the thermocline region. Another source of error is the large scatter of EOF amplitudes *versus* SST measurements. The EOF basis functions were calculated separately for the Frontal water mass region. This moved the region of EOF amplitude variability to the location of the thermocline. Synthetic profiles had slight differences in trends as the number of EOF components was increased. Disagreement still occured in the mixed layer and thermocline regions. No large improvements resulted from the tailoring of the EOF decomposition to the Frontal water mass regions. The Frontal region exhibits severe variability in structure with water mass changes along a wide span of TS curves. More investigations on the EOF representation of the Frontal water mass structures will have to be conducted with perhaps the invocation of a feature model.

The work does demonstrate, however, that it is feasible to derive synthetic temperature profiles and sound speed distributions below the surface from SST observations in some sections of a frontal region when the EOF have been computed at a particular time and place. The approach can be extended to other times of the year and seasons for which regional *in situ* data is available.

References

[1] Cheney, R.E. (1982). Comparison data for SEASAT altimetry in the western North Atlantic. *Journal of Geophysical Research*, **87**, 3247-3253.

[2] Khedouri, E., Szczechowski, C. (1983). Potential oceanographic applications of satellite altimetry for inferring subsurface thermal stucture. Oceans 83, Proc. Mar. Technol. Soc., 274-280.

[3] DeWitt, P.W. (1987). Modal decomposition of the monthly Gulf Stream, Kuroshio temperature fields. NOO Techn. Rep. 298, Naval Oceanographic Office, Stennis Space Center, Miss.

[4] Carnes, M.R., Mitchell, J.L, DeWitt, P.W. (1990). Synthetic temperature profiles derived from Geosat altimetry: Comparison with air-dropped expendable bathythermograph profiles. *Journal of Geophysical Research*, **95**, 17979-17992.

[5] Pistek, P., Mitchell, J.L., Carnes, M.R. (1993). North West Atlantic synthetic data time series. Private communication in form of finished manuscript.

[6] Boissier, C., Bouxin, H. (1991). Radar altimetry and acoustic prediction. *In:* J. Potter and A. Warn-Varnas (*eds.*): Ocean Variability and Acoustic Propagation. Dordrect, Kluwer Academic Publishers.

[7] Cummings, J.A. (1993). Water mass empirical orthogonal functions in the NW Atlantic with application to optimal field estimation. Private communication in form of finished manuscript.

[8] Fiedler, P.C. (1988). Surface manifestation of subsurface thermal structure in the California Current. *Journal of Geophysical Research*, **93**, 4975-4983.

[9] Essen, H.H., Sellschopp, J. (1994). Three-dimensional distribution of sound speed in the Iceland-Faeroe area, retrieved from a CTD survey, thermistor-chain measurements and satellite SST imagery, SACLANTCEN SR-226. La Spezia, Italy, NATO SACLANT Undersea Research Centre.

[10] Essen, H.-H. (1996). On the predictability of subsurface sound speed from satellite-measured sea-surface temperature in the Mediterranean, SACLANTCEN SR-245. La Spezia, Italy, NATO SACLANT Undersea Research Centre.

[11] Niiler, P.P, Piacsek, S., Neuberg, L., Warn-Varnas, A. (1992). Sea surface temperature variability of the Iceland-Faeroe Front. *Journal of Geophysical Research*, **97**, 17777-17785.

[12] Read, J.F., Pollard, R.T. (1992). Water masses in the region of the Iceland-Faeroe Front. *Journal of Physical Oceanography*, **22**, 1365-1378.

[13] Gandin, L.S. (1965) Objective analysis of meteorological fields. Israel program for scientific publications, Jerusalem.

[14] Carter, E.F, Robinson, A.R. (1987). Analysis models for the estimation of oceanic fields. *Journal of Atmoshperic and Oceanic Technology*, **4**, 49-74.

[15] Miller, A.J., Arango, H.G., Robinson, A.R., Leslie, W.G., Poulain, P.M., Warn-Varnas, A. (1995). Quasigeostrophic forcasting and physical processes of the Iceland-Faeroe Frontal variability. *Journal of Physical Oceanography*, **25**, 1274-1295.

[16] Minnett, P.J. (1990). The regional optimization of infrared measurements of sea-surface temperature from space. *Journal of Geophysical Research*, **95**, 13497-13510.

[17] Poulain, P.-M., Warn-Varnas, A., Niiler, P.P. (1995). Near-surface circulation of the Nordic Seas as measured by Lagrangian drifters. *Journal of Geophysical Research*, accepted.

Report no.changed (Mar 2006): SR-246-UU

Document Data Sheet

Security Classification		Project No.
		04
Document Serial No.	**Date of Issue**	**Total Pages**
SR-246	January 1996	30 pp.

Author(s)

A. Warn-Varnas, H.-H. Essen, E. Gezgin

Title

Deduction of synthetic temperature profiles from SST observations in the Iceland-Faeroe frontal region

Abstract

Subsurface temperature and sound speed profiles are generated from satellite SST observations and validated by hydrocast observations. Hydrographic data from the October 1992 Iceland Faeroe frontal survey is used for the calculation of Empirical Orthogonal Functions (EOFs). Statistical relationships between the EOF amplitudes and SSTs are derived and used for the construction of synthetic temperature profiles and sound speed distributions in the ocean. Average Root-Mean Square (RMS) errors were computed for synthetic temperature profiles in typical water categories. Corrections to the processed satellite SST data were applied using surface drifter data and sensitivity tests.

The survey data reflects the water mass structure in three distinct regions; Atlantic, Frontal and Arctic, for which characteristic TS curves are derived. The best agreement between the synthetically generated temperature profiles, from SST data, with CTD measurements occurs in the Arctic region where a tendency to follow the slope and magnitude *versus* depth exists. The Frontal region shows disagreements in the upper thermocline with agreement elsewhere. In the Atlantic region there is agreement only in the upper mixed layer. In the thermocline regime the slope exhibits a parallel offset relative to the data. The differences are attributed to the inherent errors of EOF reconstruction which peak in the thermocline and the scatter of EOF amplitudes *versus* SST measurements.

The work demonstrates that it is possible to derive synthetic temperature and sound speed profiles in the ocean from SST observations of particular water mass configurations at certain times of the season.

Keywords

Iceland-Faeroe frontal region – sea-surface temperature – temperature profiles

Issuing Organization

North Atlantic Treaty Organization
SACLANT Undersea Research Centre
Viale San Bartolomeo 400, 19138 La Spezia, Italy

[From N. America: SACLANTCEN CMR-426 (New York) APO AE 09613]

Tel: +39 (0)187 540 111
Fax:+39 (0)187 524 600

E-mail: library@saclantc.nato.int

Initial Distribution for SR-246

Ministries of Defence

DND Canada	10
CHOD Denmark	8
MOD Germany	15
HNDGS Greece	12
MARISTAT Italy	10
MOD (Navy) Netherlands	12
NDRE Norway	10
MOD Spain	2
MDN Portugal	5
TDKK Turkey	5
MOD UK	20
ONR US	49

NATO Authorities

NAMILCOM	2
SACLANT	3
CINCEASTLANT/ COMNAVNORTHWEST	1
CINCIBERLANT	1
CINCWESTLANT	1
COMASWSTRIKFOR	1
COMMAIREASTLANT	1
COMSTRIKFLTANT	1
COMSUBACLANT	1
SACLANTREPEUR	1
SACEUR	2
CINCNORTHWEST	1
CINCSOUTH	1
COMEDCENT	1
COMMARAIRMED	1
COMNAVSOUTH	1
COMSTRIKFORSOUTH	1
COMSUBMED	1
SHAPE Technical Centre	1
PAT	1

SCNR for SACLANTCEN

SCNR Belgium	1
SCNR Canada	1
SCNR Denmark	1
SCNR Germany	1
SCNR Greece	1
SCNR Italy	1
SCNR Netherlands	1
SCNR Norway	1
SCNR Portugal	1
SCNR Spain	1
SCNR Turkey	1
SCNR UK	1
SCNR US	2
SECGEN Rep. SCNR	1
NAMILCOM Rep. SCNR	1

National Liaison Officers

NLO Canada	1
NLO Denmark	1
NLO Germany	1
NLO Italy	1
NLO Netherlands	1
NLO UK	1
NLO US	1

Total external distribution	205
SACLANTCEN Library	20
Total number of copies	225